INTERNATIONAL JOURNAL FOR NUMERICAL METHODS IN FLUIDS, VOL. 11, 247–259 (1990)

# THE NUMERICAL SOLUTION OF THE LAMINAR FLOW IN A CONSTRICTED CHANNEL AT MODERATELY HIGH REYNOLDS NUMBER USING NEWTON ITERATION

ROLAND HUNT

*Department of Mathematics, University of Strathclyde, Glasgow, U.K.*

## SUMMARY

The numerical solution of the flow in a stepped channel constricted to half its width has been obtained for Reynolds numbers up to 2000 using Newton's iteration to solve the ensuing algebraic system. In order to avoid high-frequency errors, a locally fine grid is effected near the corner by transformation of the independent variables. The results predict a downstream recirculation region, observed in experiments but not found in earlier numerical calculations. The inclusion of the Dennis–Hudson upwinding, added for stability in SOR methods, whilst giving the same characteristics of the flow, is less accurate by at least an order of magnitude.

KEY WORDS Laminar flow Newton iteration Artificial viscosity

## INTRODUCTION

The numerical solution of the flow in a constricted stepped channel (Figure 1(i)) was originally performed by Dennis and Smith using a uniform grid.[1] They, however, did not find a downstream recirculation region caused by the flow separating at the corner, observed experimentally (private communication), although there is a hint of its existence on their finest grids when the Reynolds number is larger than 1000. In this paper we use a non-uniform grid which is capable of resolving this region by using a locally fine mesh. For accuracy reasons it is also necessary to have a locally fine mesh near the corner since this is a re-entrant angle which gives rise to a singularity in the vorticity. A second reason for this study is to test how the Dennis–Hudson artificial viscosity,[2] used by Dennis and Smith,[1] affects accuracy.

The algebraic system of equations resulting from differencing the governing streamfunction/vorticity equations can be solved iteratively using the Gauss–Seidel method (or, if overrelaxation is incorporated, the SOR method). For such a method to converge it is required that the ensuring Jacobian matrix is diagonally dominant. However, at large Reynolds number this often is not the case and, in order to maintain diagonal dominance, an artificial viscosity is added. This artificial viscosity, known as upwinding, should be applied in such a way that the overall accuracy of the numerical solution is maintained. The upwind difference scheme of Dennis and Hudson is particularly attractive, since not only is second-order accuracy of the equations maintained, but the artificial viscosity is applied differentially at each grid point. That is, the amount of viscosity applied is the minimum that is required locally. However, if $h$ is a typical grid spacing and $Re$ is the Reynolds number, second-order accuracy is only strictly maintained if $hRe \ll 1$, whereas the

0271–2091/90/100247–13$06.50

*Received May 1989*
*Revised November 1989*

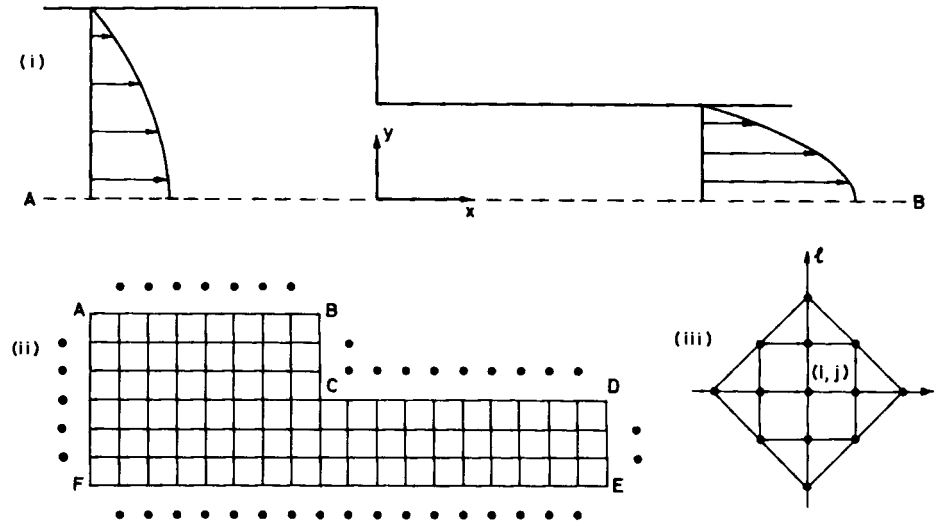


Figure 1. (i) Geometry of the stepped channel showing parabolic inflow and outflow. Only the upper half is shown since the channel is symmetrical about AB. (ii) Uniform grid in $(\xi, \eta)$ co-ordinates showing the fictitious nodes as solid circles. (iii) The 13-point molecule which is employed at each interior node

Dennis–Hudson scheme is often used to solve flows in which $hRe \gg 1$. For this reason there is some doubt as to the reliability and accuracy of the results when the Reynolds number is large.

Such iterative methods have been used in the past because computer time and storage requirements of, for example, Newton's method with its huge Jacobian matrix were greatly in excess of that provided by the computers of the day. However, with modern computers with faster central processing and enhanced storage capabilities, the direct inversion of the Jacobian becomes possible, particularly if parallel processing is available. For example, Fornberg has solved the fluid flow past a cylinder using Newton's method by exploiting the vector capabilities of a Cyber 205.[3] Since we can solve a fluid problem using a method which does not need artificial viscosity, it is possible to compare the results with and without artificial viscosity and hence to assess the effect that upwinding has on the solution. In a recent paper, Bramley and Sloan have made comparison between the results obtained with and without artificial viscosity for three tests problems which have a known analytical solution.[4] On their finest grid ($80 \times 80$), typical errors in both streamfunction and vorticity when artificial viscosity was excluded were in the range $10^{-6}$–$10^{-5}$. However, when upwinding was included these errors increased by three or four orders of magnitude and, furthermore, did not decrease as the grid spacing became finer, as one would anticipate for a second-order method. The problems considered by Bramley and Sloan were artificial in the sense that they did not represent any real flow. However, the problem considered here is a real flow.

## TRANSFORMATION OF THE EQUATIONS AND NUMERICAL TECHNIQUE

### *Governing equations*

The boundary of the flow is shown in Figure 1(i), with co-ordinates $x$ along the channel in the downstream direction, $y$ perpendicular to it and with no dependence on the third dimension. Upstream the channel lies between the planes $y = \pm 1$ and is constricted at $x = 0$ to lie between

the planes $y = \pm\frac{1}{2}$. Upstream we suppose that parabolic Poiseuille flow prevails and that far enough downstream the flow will again be parabolic. Owing to the symmetry of the flow about $y = 0$, it is only necessary to seek a solution for $y \geqslant 0$.

The Navier–Stokes equations in the streamfunction/vorticity formulation are

$$\nabla^2\psi = -\zeta, \qquad \nabla^2\zeta = Re\left(\frac{\partial\psi}{\partial y}\frac{\partial\zeta}{\partial x} - \frac{\partial\psi}{\partial x}\frac{\partial\zeta}{\partial y}\right), \tag{1}$$

where $\nabla^2$ is the Laplacian operator and $\psi$ and $\zeta$ are the streamfunction and vorticity respectively. These are related to the velocity components $(u, v)$ in the $(x, y)$ directions via

$$u = \frac{\partial\psi}{\partial y}, \qquad v = -\frac{\partial\psi}{\partial x}, \qquad \zeta = \frac{\partial v}{\partial x} - \frac{\partial u}{\partial y}. \tag{2}$$

The boundary conditions are

$$\begin{aligned} &\psi = 1, \quad \frac{\partial\psi}{\partial y} = 0 \quad \text{on } y = 1, x \leqslant 0 \text{ and } y = \tfrac{1}{2}, x \geqslant 0, \\ &\psi = 1, \quad \frac{\partial\psi}{\partial x} = 0 \quad \text{on } x = 0, \tfrac{1}{2} \leqslant y \leqslant 1, \\ &\psi = 0, \quad \frac{\partial^2\psi}{\partial y^2} = 0 \quad \text{on } y = 0. \end{aligned} \tag{3}$$

The conditions on $y=0$ preserve the symmetry of the flow and the other conditions reflect the no-slip condition.

*Transformation of the equations*

Anticipating the need for a finer grid at the corner, we make the transformations

$$x = f(\xi), \qquad y = g(\eta), \tag{4}$$

which give equations (1) as

$$\nabla^2\psi = -\zeta, \qquad \nabla^2\zeta = \frac{Re}{f'g'}\left(\frac{\partial\psi}{\partial\eta}\frac{\partial\zeta}{\partial\xi} - \frac{\partial\psi}{\partial\xi}\frac{\partial\zeta}{\partial\eta}\right), \tag{5}$$

where

$$\nabla^2 \equiv \frac{\partial^2}{\partial x^2} + \frac{\partial^2}{\partial y^2} = \frac{1}{(f')^2}\frac{\partial^2}{\partial\xi^2} - \frac{f''}{(f')^3}\frac{\partial}{\partial\xi} + \frac{1}{(g')^2}\frac{\partial^2}{\partial\eta^2} - \frac{g''}{(g')^3}\frac{\partial}{\partial\eta}. \tag{6}$$

In the $\xi$–$\eta$ plane a uniform grid is placed over the domain (see Figure 1(ii)), with an $N_1 \times M_1$ grid before the corner and an $N_2 \times M_2$ after, and we choose $M_2 = M_1/2$. The grid vertices are labelled $(i, j)$, $i = -N_1, -N_1+1, \ldots, N_2$, $j = 0, 1, \ldots, M$, where $M = M_1$ for $i \leqslant 0$ and $M = M_2$ for $i > 0$. Each element of the grid is square with dimension $h = 1/M_1$. The transformations used in the computations are

$$f(\xi) = \frac{\Delta x_0}{kh}\sinh(k\xi), \qquad g(\eta) = \eta + \frac{1}{2\pi}\left(1 - \frac{\Delta y_0}{h}\right)\sin(2\pi\eta), \tag{7}$$

where $\Delta x_0$ and $\Delta y_0$ are the dimensions of a cell in the $x$–$y$ plane next to the corner and $k$ is a parameter determined by the position of the upstream boundary. With this transformation the

boundary conditions for equations (5) are the same as (3) if $x$ and $y$ are replaced by $\xi$ and $\eta$ respectively.

It was found by numerical experimentation that, for the values of $Re$ of interest ($125 \leqslant Re \leqslant 2000$), $\Delta x_0$ has to be small otherwise the solutions are contaminated by high-frequency oscillatory modes. Demanding that the vorticity should be free of such modes, it was found that, for the finest grid used, $\Delta x_0 = 0{\cdot}00625/\sqrt{(Re)}$ is a suitable value. Ideally one would like $\Delta y_0 = \Delta x_0$, but unfortunately the Newton iteration employed did not converge for this configuration. The smallest value of $\Delta y_0$ that could be used is 0·005, which is about $20\Delta x_0$ at $Re = 500$. The probable reason for lack of convergence using small $\Delta y_0$ is the creation of long, thin rectangles at large $x$. It was found that a suitable value for the upstream boundary is $x = -4$. Downstream, however, the flow changes only slowly and this boundary is set at $x \simeq 1000$. The actual grid used for $Re = 500$ is shown in Figure 2.

*Differencing the equations*

Replacing $\partial\psi/\partial y$ and $\partial\psi/\partial x$ by $u$ and $-v$ as in equations (2), the second of equations (5) becomes

$$\frac{1}{(f')^2}\left(\frac{\partial^2\zeta}{\partial\xi^2} - A\frac{\partial\zeta}{\partial\xi}\right) + \frac{1}{(g')^2}\left(\frac{\partial^2\zeta}{\partial\eta^2} - B\frac{\partial\zeta}{\partial\eta}\right) = 0, \tag{8}$$

where $A = Re\, uf''/g' + f'''/f'$ and $B = Re\, vg'/f' + g''/g'$. Replacing derivatives by the usual central differences

$$\frac{\partial^2\zeta}{\partial\xi^2} \simeq \frac{1}{h^2}(\zeta_{i+1,j} - 2\zeta_{ij} + \zeta_{i-1,j}), \qquad \frac{\partial\zeta}{\partial\xi} \simeq \frac{1}{2h}(\zeta_{i+1,j} - \zeta_{i-1,j}), \tag{9}$$

$$\frac{\partial^2\zeta}{\partial\eta^2} \simeq \frac{1}{h^2}(\zeta_{i,j+1} - 2\zeta_{ij} + \zeta_{i,j-1}), \qquad \frac{\partial\zeta}{\partial\eta} \simeq \frac{1}{2h}(\zeta_{i,j+1} - \zeta_{i,j-1}),$$

the discretized equation corresponding to equation (8) is

$$\frac{1}{(hf_i')^2}[1 - \tfrac{1}{2}hA_{ij}]\zeta_{i+1,j} + \frac{1}{(hf_i')^2}[1 + \tfrac{1}{2}hA_{ij}]\zeta_{i-1,j} + \frac{1}{(hg_j')^2}[1 - \tfrac{1}{2}hB_{ij}]\zeta_{i,j+1}$$
$$+ \frac{1}{(hg_j')^2}[1 + \tfrac{1}{2}hB_{ij}]\zeta_{i,j-1} - \frac{2}{h^2}\left[\frac{1}{(f_i')^2} + \frac{1}{(g_j')^2}\right]\zeta_{ij} = 0. \tag{10}$$

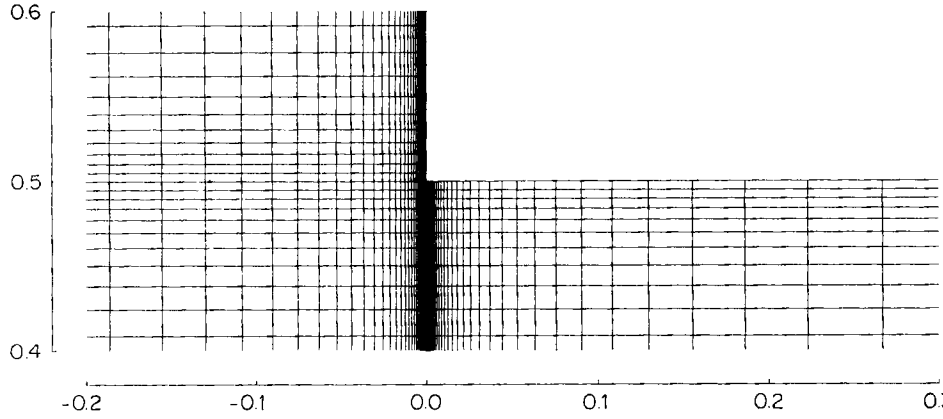


Figure 2. The actual grid used for $Re = 500$ in $(x, y)$ co-ordinates

The local truncation error is $O(Reh^2)$ and hence (10) is second-order accurate and is diagonally dominant provided the terms in square brackets remain positive, that is if $h|A_{ij}|<2$ and $h|B_{ij}|<2$. However, for large $Re$ both $A$ and $B$ will be large and these conditions for dominance will be violated, with the consequence that if an SOR iteration is used to solve the system (10), it will not converge.

*The Dennis–Hudson artificial viscosity*

In order to maintain diagonal dominance for all values of $Re$, Dennis and Hudson suggested the addition of an extra term to equation (8), namely

$$\lambda h^2\left[\frac{A^2}{(f')^2}\frac{\partial^2\zeta}{\partial\xi^2}+\frac{B^2}{(g')^2}\frac{\partial^2\zeta}{\partial\eta^2}\right]. \tag{11}$$

Since this is proportional to $h^2$, the accuracy of the resulting difference scheme will still be second-order, and since the nature of the term is 'viscous', it is usually referred to as artificial or numerical viscosity. Differencing (11) using equations (9) and adding to (10) gives

$$\begin{aligned}&\frac{1}{(hf_i')^2}[1-\tfrac{1}{2}hA_{ij}+\lambda h^2A_{ij}^2]\zeta_{i+1,j}+\frac{1}{(hf_i')^2}[1+\tfrac{1}{2}hA_{ij}+\lambda h^2A_{ij}^2]\zeta_{i-1,j}\\&+\frac{1}{(hg_j')^2}[1-\tfrac{1}{2}hB_{ij}+\lambda h^2B_{ij}^2]\zeta_{i,j+1}+\frac{1}{(hg_j')^2}[1+\tfrac{1}{2}hB_{ij}+\lambda h^2B_{ij}^2]\zeta_{i,j-1}\\&+\frac{2}{h^2}\left[\frac{1}{(f_i')^2}\{1+\lambda h^2A_{ij}^2\}+\frac{1}{(g_j')^2}\{1+\lambda h^2B_{ij}^2\}\right]\zeta_{ij}=0.\end{aligned} \tag{12}$$

Diagonal dominance is maintained provided the terms in square brackets are positive, that is for $\lambda>\frac{1}{16}$. For robustness it is desirable to choose $\lambda$ a little away from $\frac{1}{16}$ and in practice $\lambda$ is set to $\frac{1}{8}$, although Bramley and Sloan choose $\frac{1}{12}$. In this paper we will set $\lambda$ to $\frac{1}{8}$. The local truncation error is now $O(Re^2h^2)$ and, although technically second-order, will not be as accurate as (10) for large $Re$. Clearly, equations (12) include the case of no artificial viscosity by setting $\lambda=0$, thus reverting to equations (10).

*The system of equations to be solved*

The first of equations (5) is differenced as

$$\begin{aligned}&\frac{1}{(hf_i')^2}(1-\tfrac{1}{2}ha_i)\psi_{i+1,j}+\frac{1}{(hf_i')^2}(1+\tfrac{1}{2}ha_i)\psi_{i-1,j}+\frac{1}{(hg_j')^2}(1-\tfrac{1}{2}hb_j)\psi_{i,j+1}\\&+\frac{1}{(hg_j')^2}(1+\tfrac{1}{2}hb_j)\psi_{i,j-1}-\frac{2}{h^2}\left[\frac{1}{(f')^2}+\frac{1}{(g')^2}\right]\psi_{ij}=-\zeta_{ij}.\end{aligned} \tag{13}$$

where $a=f''/f'$ and $b=g''/g$. By substituting this into (12) for each $\zeta_{k,l}$ and using

$$u_{ij}=\frac{1}{2hf_i'}(\psi_{i+1,j}-\psi_{i-1,j}),\qquad v_{ij}=-\frac{1}{2hg_j'}(\psi_{i,j+1}-\psi_{i,j-1}) \tag{14}$$

to replace $u_{ij}$ and $v_{ij}$, the only dependent variable in equations (12) will be $\psi_{k,l}$. At a given location $(i,j)$ these $\psi_{k,l}$ will form the 13-point molecule as shown in Figure 1(iii). To accommodate the boundary conditions, fictitious nodes are used as shown in Figure 1(ii) and then the boundary

equations are

$$\begin{aligned}
\psi_{i,M_1} &= 1, \quad \psi_{i,M_1+1} = \psi_{i,M_1-1} \quad \text{on AB,} \\
\psi_{0,j} &= 1, \quad \psi_{1,j} = \psi_{-1,j} \quad \text{on BC,} \\
\psi_{i,M_2} &= 1, \quad \psi_{i,M_2+1} = \psi_{i,M_2-1} \quad \text{on CD,} \\
\psi_{N_2,j} &= \psi_{N_2+1,j} = y_j(3-4y_j^2) \quad \text{on DE,} \\
\psi_{i,0} &= 0, \quad \psi_{i,-1} = -\psi_{i,1} \quad \text{on EF,} \\
\psi_{-N_1,j} &= \psi_{-N_1-1,j} = \tfrac{1}{2}y_i(3-y_i^2) \quad \text{on FA,}
\end{aligned} \tag{15}$$

where Poiseuille flow has been assumed on boundaries DE and FA and their associated fictitious nodes. The fictitious node at C is defined in two different ways depending on whether the molecule is at $(-1, M_2+1)$, which uses the second condition, or at $(1, M_2-1)$, which uses the third. The system of equations from which a solution to the problem will be obtained is found by applying the 13-point molecule to each interior point and replacing $\psi_{k,l}$ on the boundary and in the fictitious nodes using (15). Hence the unknowns in these equations are the $\psi_{ij}$ at interior points only and consequently the number of unknowns equals the number of equations. We write this system of equations as

$$\mathbf{F}(\Psi) = 0, \tag{16}$$

where $\Psi^{\mathrm{T}} = (\psi^{\mathrm{T}}_{-N_1+1}, \psi^{\mathrm{T}}_{-N_1+2}, \ldots, \psi^{\mathrm{T}}_{N_2-1})$ with $\psi_i^{\mathrm{T}} = (\psi_{i,1}, \psi_{i,2}, \ldots, \psi_{i,M-1})$, where $M = M_1$ for $i < 0$ and $M = M_2$ for $i \geqslant 0$. Thus F and $\Phi$ are vectors of length $(N_1-1)(M_1-1)+N_2(M_2-1)$.

*Newton's iteration*

Equation (16) is to be solved using Newton's method, which can be written as

$$\mathbf{J} = \partial \mathbf{F}(\Psi^{(s)})/\partial \Psi, \tag{17}$$

$$\mathbf{J}\Delta\Psi^{(s)} = -\mathbf{F}(\Psi^{(s)}), \qquad s = 0, 1, 2, \ldots, \tag{18}$$

$$\Psi^{(s+1)} = \Psi^{(s)} + \Delta\Psi^{(s)}, \tag{19}$$

where J is the Jacobian of the system and $\Psi^{(s)}$ is the $s$th iterate. Each iteration consists of three steps, namely calculating the Jacobian (17), inverting the matrix equation (18) and updating the solution (19).

It is more efficient to calculate the Jacobian algebraically. However, the use of transformation (7) in the equations made this prohibitively difficult and hence the elements of J are calculated dynamically via the formula

$$J_{kl,ij} = \frac{\partial F_{kl}}{\partial \psi_{ij}} \simeq \frac{1}{\varepsilon}[F_{kl}(\ldots, \psi_{ij}+\varepsilon, \ldots) - F_{kl}(\ldots, \psi_{ij}, \ldots)], \tag{20}$$

where $\varepsilon$ is a small quantity set to $10^{-6}$. Equation (20) therefore calculates J to approximately six decimal places, which is sufficient for the Newton iteration to converge rapidly. $J_{kl,ij} = 0$ except when $|k-i|+|l-j| \leqslant 2$, and hence for each row of J there are at most 13 non-zero elements. The form of the matrix J is shown in Figure 3.

Equation (18) is solved by using Gaussian elimination. A code was written to take advantage of the special nature of the matrix J; that is, a banded matrix whose band width changes from $4M_1-3$ to $4M_2-3$ after location $(N_1-1)(M_1-1)+M_2$ (see Figure 3). This greatly increases the efficiency of the program. The code was written with and without partial pivoting and was

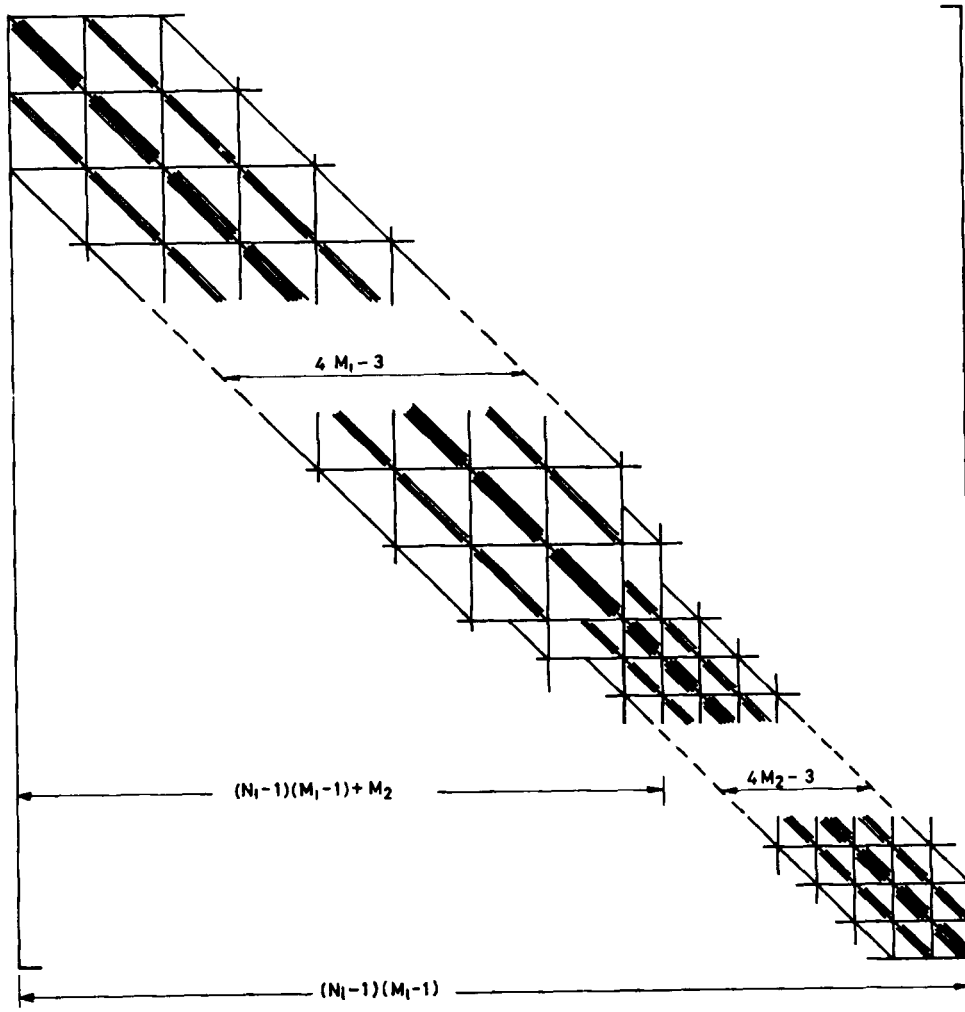


Figure 3. The form of the Jacobian matrix J showing the non-zero elements and the banded structure

found to work perfectly well without pivoting. The main storage requirement of the program is the banded section of **J** ($\sim 8 \times 10^5$ locations for the largest array used), which can be stored in single precision since **J** is only accurate to this level. This, coupled with non-pivoting, enabled us to employ the array sizes cited in the *Implementation* section, which were the maximum allowable at the installation this work was carried out.

Calculating **J** and its subsequent inversion is very time-consuming and it was found preferable to use a modification of Newton's method in which **J** is fixed after a few iterations. Thus for $s > m$ equation (17) is replaced by

$$\mathbf{J} = \partial \mathbf{F}(\mathbf{\Psi}^{(m)})/\partial \mathbf{\Psi}, \tag{21}$$

which has already been calculated. Further, after forward elimination, the reduced form of **J**, which is upper triangular, is stored on and above the main diagonal of the matrix shown in

Figure 3, with the associated multipliers (used in the elimination process) stored below the diagonal. Hence it is only necessary to apply these multipliers to the right-hand side of (18) and then $\Delta\Psi^{(s)}$ is obtainable by back-substitution in the usual way. For the largest array used the full iteration took $\sim 95$ s compared with $\sim 2{\cdot}5$ s for the fixed iteration on a VAX 8650. It was found that setting $m = 1$ (i.e. two full iterations) is adequate to give reasonably rapid convergence using the fixed iteration. Typically 10–15 fixed iterations were required for convergence.

*Woods' boundary condition and corner treatment*

In order to solve the system of equations using SOR iteration, it is necessary to know the vorticity $\zeta$ on the boundary. This is usually obtained using the Woods' boundary condition.[5] Suppose the boundary in question is $\eta =$ constant with $\psi_1$ and $\psi_0$ the values of $\psi$ next to and on the boundary; then using a Taylor expansion we can express $\psi_1$ in terms of $\psi_0$ as

$$\psi_1 = \psi_0 - h\frac{\partial\psi}{\partial\eta}\bigg|_0 + \tfrac{1}{2}h^2\frac{\partial^2\psi}{\partial\eta^2}\bigg|_0 + \tfrac{1}{6}h^3\frac{\partial^3\psi}{\partial\eta^3}\bigg|_0 + O(h^4). \tag{22}$$

Using the first of equations (5) to replace $\partial^2\psi/\partial\eta^2$ and then approximating $\partial\zeta/\partial\eta$ by $(\zeta_0-\zeta_1)/h+O(h)$ and noting that $g_0''=0$ if (7) is used, we have

$$\zeta_0 = \frac{3}{(hg')^2}(\psi_0-\psi_1)-\tfrac{1}{2}\zeta_1 + O(h^2). \tag{23}$$

Neglecting the $O(h^2)$ term, (23) gives a value for $\zeta$ on the boundary which is second-order accurate and is the Woods' boundary condition modified by transformation (7). Truncating (22) after the $h^2$ term gives the first-order-accurate estimate for $\zeta$ on the boundary as

$$\zeta_0 = \frac{2}{(hg')^2}(\psi_0-\psi_1)+O(h). \tag{24}$$

Neglecting the $O(h)$ term and using (13) to replace $\zeta_0$ in terms of the five-point molecule in $\psi$, we find that (24) is identical to the conditions stated in (15). It is well known that second-order accuracy is maintained even when a first-order boundary condition is employed. Hence conditions (15), which are second-order in $\psi$ but only first-order in $\zeta$, will give second-order-accurate results in both $\psi$ and $\zeta$. However, for the sake of completeness, we will also consider the effect of the more accurate boundary condition given by (23).

Another difficulty encountered when using an SOR iteration is how to deal with the infinite vorticity at the corner. Several techniques have been proposed to overcome this,[1,6] of which we shall consider two. Firstly, the five-point molecule used to approximate the $\nabla^2$ operator is rotated through 45° at points near the corner in such a way that the value of the vorticity at the corner is never used. The second approach is to use a Moffatt expansion at the corner. One can show that close to the corner the right-hand side of the second of equations (1) can be neglected compared to the right-hand side. Moffatt's solution[7] can then be applied in the neighbourhood of the corner to estimate the vorticity. For a re-entrant angle of 270° this is

$$\zeta = Ar^{-0{\cdot}45552}\cos(0{\cdot}45552\,\theta) + Br^{-0{\cdot}09147}\sin(0{\cdot}09147\,\theta), \tag{25}$$

where $r, \theta$ are the polar co-ordinates centred at the corner, with $\theta$ measured from the line of symmetry, and $A$ and $B$ are constants. This difficulty is not encountered in Newton's method since equation (16) only contains $\psi$. However, it will be appreciated that $\psi$ has singular second derivatives at the corner which will affect the accuracy of the solution.

*Implementation*

The system of equations is solved on grids having dimensions $N_1 = M_1 = 48$, $N_2 = 80$ and $M_2 = M_1/2 = 24$ (denoted by $48 \times 128$). A suitable starting solution $\Psi^{(0)}$ for Newton's iteration is obtained by a combination of continuation and grid refinement. Commencing on a $12 \times 32$ grid with $\Psi^{(0)}$ chosen to match most of the boundary conditions, a solution is found for zero Reynolds number. Then solutions are found for Reynolds numbers $Re^{r/6}$, $r = 1, 2, \ldots, 6$, with the starting solution given by the solution for the previous $Re$. The solutions are obtained for $24 \times 64$ and $48 \times 128$ grids using the starting solution given by the solution from the next coarsest grid, the values of intermediate points being obtained by cubic interpolation (linear interpolation is not accurate enough). In the continuation process a single iterate is sufficient to give a good starting solution for the next step. For the final three grids, iteration is continued until the largest element in $\Delta\Psi^{(s)}$ is less than $10^{-8}$ in magnitude. Thus for each case studied, results were obtained for three grids, namely $12 \times 32$, $24 \times 64$ and $48 \times 128$.

## RESULTS AND DISCUSSION

*Without artificial viscosity*

The flow diagrams for $Re = 125, 250, 500, 1000$ and $2000$ are shown in Figure 4, in which the artificial viscosity parameter $\lambda$ is set to zero. The error in the results can be estimated by comparing the results on the two finest grids ($48 \times 128$ and $24 \times 64$) at common locations. Since the method is second-order, the error at location $(i, j)$ is approximately

$$\tfrac{1}{3}|u_{ij}^{F} - u_{ij}^{C}|, \tag{26}$$

where F/C refer to the result on the fine/coarse grid respectively, and these errors are given in Table I. Maximum errors in the streamfunction are in the range $10^{-3}$–$10^{-2}$, with average errors a magnitude lower. These errors are quite large and are due entirely to the non-analytic nature of the solution at the corner (compare errors of $\sim 10^{-6}$ found by Bramley and Sloan using analytic functions[4]). The errors in velocity and vorticity are a magnitude higher in general, which is as expected since they are obtained by differencing the streamfunction. Interestingly, the streamfunction maximum errors are proportional to $Re$, reflecting the $O(Reh^2)$ of the truncation error.

The most interesting feature of the results is that the flow separates at the corner, forming a recirculation region downstream. This region is indicated by experiments but not found in the numerical calculations of Dennis and Smith, probably because the grid employed was not fine enough in this region. The separation first appears at $Re = 250$ and becomes larger in both length and strength as $Re$ increases, the length being roughly proportional to $Re$. The separation streamline is not attached to the corner but slightly to the right. This has been observed experimentally and is confirmed theoretically by fitting of Moffatt expansion[7] to the corner. The recirculation region in corner B is quantitatively similar to that found by Dennis and Smith. Sizes and strengths of both recirculation regions are shown in Table II. A contour map of the vorticity at $Re = 500$ is given in Figure 5, clearly showing the singularity at the corner.

*With artificial viscosity*

The Dennis–Hudson difference scheme is programmed by setting the artificial viscosity parameter $\lambda$ to $\frac{1}{8}$. The code is less robust than when $\lambda = 0$, and in fact did not converge for $Re = 1000$ and $2000$. This is surprising since one would expect the addition of a 'viscous'-like term

to have a stabilizing effect. As $Re$ increases and the grid becomes finer, convergence becomes more and more difficult, and for $Re > 500$ no convergence is possible on the finest grid. The impression given is that for these high Reynolds numbers the underlying system of equations does not have a solution.

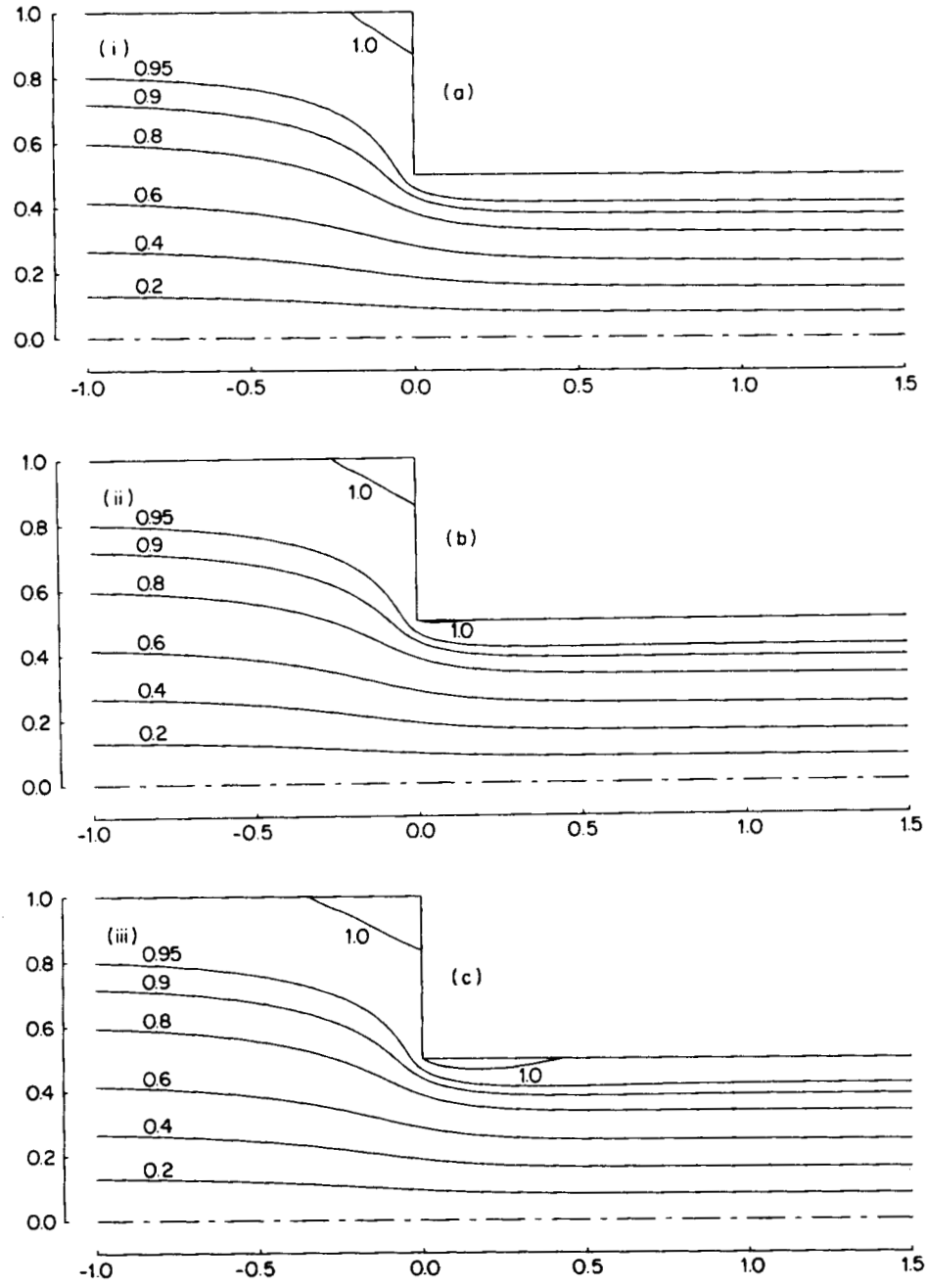


Figure 4. (a–c)

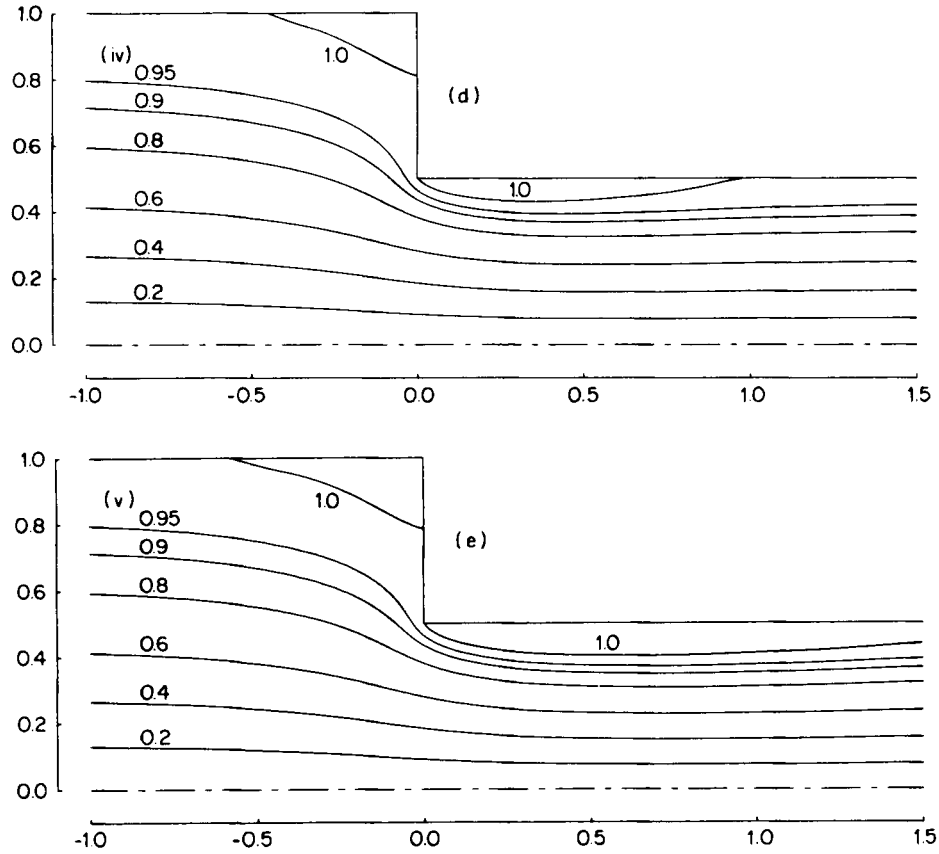


Figure 4. The streamlines of flow for Reynolds number (i) 125, (ii) 250, (iii) 500, (iv) 1000 and (v) 2000

Table I. Errors (in units of $10^3$) in the results without artificial viscosity for various Reynolds numbers

| Reynolds number | Streamfunction (absolute errors) | | Velocity magnitude (average absolute error) | Vorticity (absolute relative error) |
|---|---|---|---|---|
| | Maximum | Average | | |
| 125 | 0·56 | 0·15 | 3·1 | 13·8 |
| 250 | 1·09 | 0·19 | 3·1 | 19·8 |
| 500 | 2·03 | 0·21 | 4·0 | 28·4 |
| 1000 | 4·10 | 0·41 | 6.2 | 38·6 |
| 2000 | 8·31 | 0·62 | 8·2 | 51·6 |

For the three convergent cases ($Re$ = 125, 250 and 500) the results are characteristically similar to those for $\lambda = 0$. Both recirculation regions are found which have dimensions and strengths to within $\sim 15\%$ of those given by the zero-artificial-viscosity case (see Table II). In contrast, the accuracy of the results is less good. Table III shows that the overall error is at least a magnitude

Table II. Dimensions and strengths of the two recirculation regions without artificial viscosity and with artificial viscosity (in parentheses). The last column gives the distance from the corner of the downstream recirculation region

| | Upstream recirculation region | | | Downstream recirculation region | | | |
|---|---|---|---|---|---|---|---|
| Reynolds number | Length | Width | Maximum $\psi$ | Length | Width | Maximum $\psi$ | Distance from corner |
| 125 | 0·168 (0·164) | 0·128 (0·126) | 1·00006 (1·00006) | — | — | — | — |
| 250 | 0·227 (0·209) | 0·145 (0·138) | 1·00014 (1·00012) | 0·096 (0·106) | 0·0107 (0·0114) | 1·00021 (1·00003) | 0·023 (0·018) |
| 500 | 0.308 (0·260) | 0·164 (0·149) | 1·00026 (1·00018) | 0·406 (0·406) | 0·0413 (0·0466) | 1·00132 (1·00152) | 0·008 (0·006) |
| 1000 | 0·394 | 0·188 | 1·00053 | 0·956 | 0·0820 | 1·00779 | 0·005 |
| 2000 | 0·507 | 0·214 | 1·00080 | 2·039 | 0·1147 | 1·01562 | 0·004 |

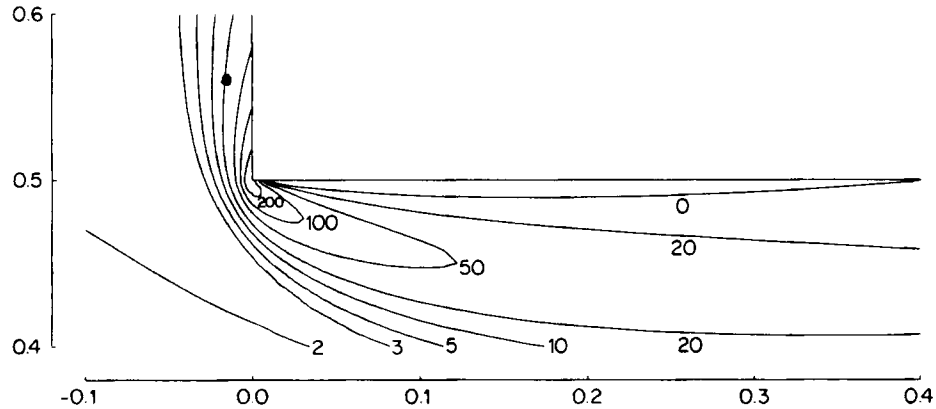


Figure 5. Viscosity contours for $Re = 500$ showing the singularity at the origin

higher than when $\lambda = 0$. Furthermore, as found by Bramley and Sloan,[4] the errors do not decrease as the grid size increases in a manner consistent with a second-order method. The ratio of the average errors from grids with sizes $48 \times 128$ and $24 \times 64$ should be 4. For $\lambda = 0$ these are close to 4 but for $\lambda = \frac{1}{8}$ they are considerably less than 4, indicating that the method is closer to a first-order method than a second-order one. The largest errors do not appear to be associated with the corner but occur downstream. These errors should therefore be regarded as a consequence of applying the Dennis–Hudson viscosity to a high-Reynolds-number flows.

*Woods' boundary condition and corner treatment*

For these special treatments used in SOR iterations, the average errors are shown in Table III for the single case $Re = 500$. As expected, the Woods' boundary condition, being second-order, does not affect the overall accuracy of the result and the flow diagrams are in fact very similar. However, the use of molecule rotation or a Moffatt expansion (used to avoid using the infinite vorticity at the corner) gave much less accurate results and the order of the method no longer

Table III. Average absolute error in the streamfunction of the standard results without artificial viscosity, results with the artificial viscosity constant $\lambda = \frac{1}{8}$ and special cases. The error ratio is that compared with the standard results and the order is the perceived order calculated from the ratio of the errors of the results on the two finest grids

| | Reynolds number | Error $\times 10^4$ | Error ratio | Order |
|---|---|---|---|---|
| Standard program | 125 | 1·5 | | 2·02 |
| | 250 | 2·0 | | 2·05 |
| | 500 | 2·1 | | 2·09 |
| Dennis–Hudson artificial viscosity | 125 | 20·7 | 13·8 | 1·36 |
| | 250 | 40·1 | 20·6 | 1·28 |
| | 500 | 68·0 | 32·1 | 0·40 |
| Woods' boundary condition | 500 | 3·3 | 1·6 | 2·30 |
| 45° molecule rotation | 500 | 14·9 | 7·0 | 1·12 |
| Moffatt expansion | 500 | 22·8 | 10·8 | 1·52 |

appears to be two. This is rather surprising since both have been used successfully in other contexts. The use of long, thin rectangles near the corner is the probable cause of these errors. Molecule rotation is unnatural unless the grid aspect ratio is 1, and Moffatt's solution is determined by the vorticity at positions nearest the corner along the boundaries, which, having a long aspect ratio, could distort the solution.

## CONCLUSIONS

Newton iteration can be successfully used to obtain the high-Reynolds-number flow in a stepped channel to reasonable accuracy considering the difficulties encountered by the corner. To avoid high-frequency error modes contaminating the solution, it is necessary to have a refined grid near the corner, which is affected by a suitable algebraic transformation of the independent variables. The code, both with and without artificial viscosity, successfully, predicts a secondary, downstream recirculation region, observed in experiments but not found in previous calculations. This success is because the transformation enables the grid to be locally fine within the recirculation region. The Dennis–Hudson difference scheme, whilst giving the characteristics of the flow, is considerably less accurate than when artificial viscosity is excluded.

### ACKNOWLEDGEMENT

I should like to thank Dr. J. S. Bramley for introducing me to this problem and for his constant help and encouragement.

### REFERENCES

1. S. C. R. Dennis and F. T. Smith, 'Steady flow through a channel with a symmetrical constriction in the form of a step', *Proc. R. Soc. A*, **377**, 393–414 (1980).
2. S. C. R. Dennis and J. D. Hudson, 'A difference method for solving the Navier–Stokes equations', *Proc. 1st Conf. on Numerical Methods in Laminar and Turbulent Flow*, Pentech Press, London, 1978.
3. B. Fornberg, 'Steady viscous flow past a circular cylinder up to Reynolds number 600', *J. Comput. Phys.*, **61**, 297–320 (1985).
4. J. S. Bramley and D. M. Sloan, 'A comparison of an upward difference scheme with a central difference scheme for moderate Reynolds number', *Internal Report No. 3*, Department of Mathematics, Strathclyde University, 1988.
5. L. C. Woods, 'A note on the numerical solution of fourth order differential equations', *Aeronaut. Q.*, **5**, 176–184 (1954).
6. J. S. Bramley and S. C. R. Dennis, 'The numerical solution of two-dimensional flow in a branching channel', *Comput. Fluids*, **12**, 339–355 (1984).
7. H. K. Moffatt, 'Viscous and resistive eddies near a sharp corner', *J. Fluid Mech.*, **18**, 1–18 (1964).